EDGEWOOD
CHEMICAL BIOLOGICAL CENTER
U.S. ARMY SOLDIER AND BIOLOGICAL CHEMICAL COMMAND

ECBC-TR-334

CHEMICAL AGENT HYDROLYSIS ON DRY AND HUMIDIFIED ADSORBENTS

David McGarvey
John Mahle
George Wagner

RESEARCH AND TECHNOLOGY DIRECTORATE

July 2003

Aberdeen Proving Ground, MD 21010-5424

Disclaimer

The findings in this report are not to be construed as an official Department of the Army position unless so designated by other authorizing documents.

REPORT DOCUMENTATION PAGE

Form Approved
OMB No. 0704-0188

1. AGENCY USE ONLY *(Leave Blank)*	2. REPORT DATE	3. REPORT TYPE AND DATES COVERED
	2003 July	Final; 00 Aug – 03 Mar

4. TITLE AND SUBTITLE

Chemical Agent Hydrolysis on Dry and Humidified Adsorbents

5. FUNDING NUMBERS

NONE

6. AUTHOR(S)

McGarvey, David; Mahle, John; and Wagner, George

7. PERFORMING ORGANIZATION NAME(S) AND ADDRESS(ES)

DIR, ECBC, ATTN: AMSSB-RRT, APG, MD 21010-5424

8. PERFORMING ORGANIZATION REPORT NUMBER

ECBC-TR-334

9. SPONSORING/MONITORING AGENCY NAME(S) AND ADDRESS(ES)

10. SPONSORING/MONITORING AGENCY REPORT NUMBER

11. SUPPLEMENTARY NOTES

12a. DISTRIBUTION/AVAILABILITY STATEMENT

Approved for public release; distribution is unlimited.

12b. DISTRIBUTION CODE

13. ABSTRACT *(Maximum 200 words)*

This study considers the rate of reaction of GB, GD, VX, and HD on selected adsorbents measured using a solid phase NMR technique. The adsorbents in dry and humidified conditions are exposed to the chemical agents. The rate of disappearance of the starting chemical over time is used to calculate a reaction half time and first order reaction rate. The appearance of reaction product peaks are also noted. The half times for humid conditions are <800 min in all cases, but could be >10,000 min for some dry cases.

14. SUBJECT TERMS

Solid Phase NMR	Reaction rates	Carbon	HD
Molecular sieves	Silica gel	GD	VX
Activated alumina	Adsorption	GB	

15. NUMBER OF PAGES

31

16. PRICE CODE

17. SECURITY CLASSIFICATION OF REPORT	18. SECURITY CLASSIFICATION OF THIS PAGE	19. SECURITY CLASSIFICATION OF ABSTRACT	20. LIMITATION OF ABSTRACT
UNCLASSIFIED	UNCLASSIFIED	UNCLASSIFIED	UL

Blank

PREFACE

The work described in this report was started in August 2000 and completed in March 2003.

The use of either trade or manufacturers' names in this report does not constitute an official endorsement of any commercial products. This report may not be cited for purposes of advertisement.

This report has been approved for public release. Registered users should request additional copies from the Defense Technical Information Center; unregistered users should direct such requests to the National Technical Information Service.

Blank

CONTENTS

FIGURES

TABLES

Blank

CHEMICAL AGENT HYDROLYSIS ON DRY AND HUMIDIFIED ADSORBENTS

1. INTRODUCTION

1.1 Study Definition.

Microporous adsorbents are used to retain CW vapors in air purification filters. The vapors are physically adsorbed due to van der Waals forces where the extent of pore filling is directly related to adsorbate vapor pressure. Once adsorbed the vapors assume a liquid-like state. At low loadings of adsorbent the adsorbate/adsorbent interaction is large relative to the adsorbate/adsorbate interaction resulting in tremendous separation coefficients such that the mass of material in the vapor phase can be neglected. The adsorption behavior or several CW agents are considered here. These chemicals isopropyl methylphosphonoflouridate (GB), pinacolyl methylphosphonoflouridate (GD), bis-(2-chloroethyl) sulfide (mustard, HD), O-ethyl-S-(2-isopropylaminoethyl)methyl phosphothiolate (VX) are characterized as low volatility species. Therefore once adsorbed they would be difficult to remove and thus subject to long term effects such reaction and decomposition.

In most practical air purification applications coadsorption of water vapor also occurs. This results in an adsorbed phase mixture where the low volatility chemical agents are preferentially adsorbed versus water. The adsorbed phase water concentrations can exceed that of the CW compound at high relative humidity and low vapor phase agent concentrations. The presence of adsorbed water and reactive functional groups on the adsorbent tends to promote chemical reactions such as hydrolysis of the chemical agent, due to a large molar excess of adsorbed water. The extent and rate of chemical reaction is significant for filter operation to determine the effect on capacity of adsorbents. A hydrolysis rate model could be incorporated with a material balance model to predict filter performance for reactive compounds.

There are a number of adsorbents used commercially for air purification applications. All of the most common adsorbent materials have several similar characteristics. The materials are formulated into hardened particles, which are typically either granular or spherical. These adsorbents contain a large fraction of micropores to achieve high adsorption capacity. Activated carbon based adsorbents are used primarily in air purification due to the unfavorable water adsorption characteristics of the graphitic surface. Zeolites, silica gels and activated aluminas have found application in regenerative filtration. These inorganic adsorbents would likely yield even greater agent decomposition behavior due to the presence of acid sites.

This study will consider the rate of reaction of GB, GD, VX and HD on selected adsorbents measured using a solid phase NMR technique. This work will extend a series of earlier studies to consider a broader range of chemicals and adsorbents.

1.2 Adsorbed Phase Hydrolysis Review.

A number of techniques have been developed to follow the extent of adsorbed phase reactions. These fall into two categories either quenching or in situ analysis. The former could be accomplished by a solvent wash technique followed by quantification of the extract. The latter can be accomplished using spectroscopic techniques, for example infrared or NMR. The solid phase NMR probe can be used to monitor the extent and rate of reactivity of chemical agent on selected carbonaceous and inorganic adsorbents. This technique employs a small adsorbent sample subjected to high spin rates and situated at the Magic Angle. An earlier study (Wagner et al. 1995) considered the reaction of a mustard simulant on BPL carbon from the liquid phase by ^{13}C and ^{1}H MAS NMR. That work also demonstrated the incremental loading in the micropores could be observed through peak shifts representing changes in the adsorbate environment from liquid-like to pore wall influenced adsorbate. Approximately 5.5 ppm shifts were recorded for two different adsorbates. The reaction rates and product production of mustard on dry and humidified coconut shell carbon were also analyzed using ^{13}C MAS NMR (Karwacki et al. 1999a). Samples were prepared using 0.10 g/g loading on carbon samples with 0.132 g/g of water. Samples were stored for up to 110 days. The fraction of mustard remaining after that period was 71, 35.9, 32% for 30, 60 and 90 °C. The corresponding first order rate constants were determined to be 1.9×10^{-5}, 7.3×10^{-5} and 3.9×10^{-4} m^{-1} at 30, 60 and 90 °C on coconut shell carbon. These results were found to be consistent with results obtained by extraction.

Earlier studies have reported the hydrolysis rates of the compounds in this study from the aqueous phase. These results are summarized in Table 1. The rates for GD, GB and VX were reported in terms of a second order mechanism in aqueous alkali, while the present approach corresponds to pH of 7. The HD hydrolysis was reported for the Cl^- displacement in the presence of a solvent used to solubilize the HD. It should be noted that adsorbents the reaction could be product limited whereas the liquid phase results correspond to dilute behavior.

Table 1. Liquid Phase Hydrolysis Rates

Compound	$t_{½}$ (min)	T (°C)	Ref
HD	5	25	Yang (1988)
GD	10600	25	"
VX	2.2×10^{7}	22	"
GB	4260	25	"
Acetic Anhydride	8.1	25	Asprey (1996)

The hydrolysis mechanism of these compounds has been analyzed previously. The principle hydrolysis reaction pathway for HD is summarized in Figure 1. Two HD form a branched sulfonium ion $(ClCH_2CH_2)_2S^+(Cl^-)CH_2CH_2SCH_2CH_2Cl$ (1), which yields a cyclic sulfonium ion $S(CH_2CH_2)_2S^+(Cl^-)CH_2CH_2Cl$ (2), which yields one dithiane $S(CH_2CH_2)_2S$ (3). This is accompanied by the release of two 1,2-dichloroethanes, which often escape detection due to its high volatility.

Both GB and GD proceed to the acid with the possibility of forming surface bound intermediates, Figure 2. VX hydrolysis, Figure 3, proceeds through the EMPA intermediate or directly to EA-2192. A probable mechanism for acetic anhydride hydrolysis proceeds through the protonation of acetic anhydride as shown in Figure 4.

The solid phase NMR can be used to compare the reactivity of simulants versus the agents. Often it is advantageous to conduct testing of adsorption filters using non-toxic simulants however there are no universally accepted simulant chemicals because different physical or chemical properties are of interest in different studies with reaction properties similar to the chemical agents. The application of liquid drops to the surface of adsorbent particles in an NMR tube can be envisioned as a batch reactor. The progress of the reaction as recorded by NMR may be modeled using a batch reactor model.

$$\frac{\partial C_i}{\partial t} = R_i \tag{1}$$

Experimental procedures will be used to load adsorbents with a known quantity and monitor the conversion due to either thermal decomposition or hydrolysis mechanisms.

To study the implication of reaction effects on low volatility adsorbed species a symmetric non-toxic simulant will be chosen. One candidate is acetic anhydride, which will yield acetic acid upon hydrolysis. The rate and mechanism of reactions on the adsorbent will be compared to the aqueous reaction. Asprey (1996) used a temperature scanning technique to measure the rate of hydrolysis from 12-50 °C. They found that the reaction followed a second order rate expression as measured by conductivity.

$$R_i = \frac{-dC[Ac_2O]}{dt} = k'[Ac_2O][H_2O] \tag{2}$$

The reaction rate constant was calculated using an Arrhenius expression k = Aexp(-E/RT) with ln(A) of 7.5 l/gmol/s and E as 10.9 kcal/gmol. At 25 °C this corresponds to a rate constant k =1.42 x 10^{-3} s^{-1} for a water concentration of 55.5 gmol/l and a half-life of 8.1 min. This rate would be expected to be highly dependent on the water concentration in the adsorbed phase. The rate of hydrolysis will be examined as a function of water loading and temperature.

The observed rate can depend on transport resistances. It is possible to examine this effect by developing a model of combined transport and reaction, which is compared to the measured data for this simple system. Transport effects can be significant for adsorption systems. Gas phase adsorption is controlled by external film and intraparticle resistances. For the case where the sample is introduced as a liquid droplet the film resistance can be neglected. It is possible to estimate the magnitude of this intraparticle resistance from simple models of particle scale diffusion. A linear driving force model can used to describe the diffusion rate.

$$\frac{dn}{dt} = \frac{D_e}{R_p^{\,2}}(n - n^*) \tag{3}$$

The approximate value of the surface diffusion coefficient ranges from 1×10^{-3} to 1×10^{-5} cm^2/s for large pore adsorbents. However is could be much slower, 1×10^{-8} cm^2/s for zeolites if a molecule was hindered from entering the zeolite cage. The half time corresponding to uptake for a 0.1 cm diameter particle would be approximately 350 s for D_s of 1×10^{-5} cm^2/s and 35 s for D_s of 1×10^{-4} cm^2/s. This is much shorter than the half time for reaction reported earlier for HD on coconut shell carbon under both dry and humid conditions.

The effect of droplet size on reaction rates was examined (Wagner et al. 2002). Their results are presented in Table 2. For GD the most water soluble of the compounds considered no effect was seen. Greater drop size dependence was noted for the less water soluble components. These results however are difficult to interpret because the extent of hydration of the adsorbent was not well controlled. Also the rate could be limited by the amount of adsorbent. It would be better to conduct testing with a fixed adsorbed phase loading to compare results between chemicals and adsorbents.

Table 2. Effect of Drop Size on Agent Hydrolysis (Wagner et al. 2002)

Agent	Adsorbent	Drop size (µl)	Halftime (min)
GD	Al_2O_3	3.5, 16	108
VX	Al_2O_3	3.5	9360
VX	Al_2O_3	15	14076
HD	Al_2O_3	3.5	44
HD	Al_2O_3	13	4254

For the case of coadsorption of two slightly miscible reactive components then the appropriate diffusivity to consider would be an interfacial diffusion limited by product accumulation and inhibition at the interface. Clearly accurate description of this behavior is difficult to characterize.

Several adsorbents can be considered because of their wide use in air purification applications. Silica gel and activated alumina are large pore materials typically used in air drying. Activated carbon is useful for non-specific organic vapor removal. Some typical properties of the adsorbents are listed in Table 3.

Table 3. Physical Properties of Adsorbents

	Manufacturer	Pore Volume (cm^3/kg)	Surface Area (m^2)
Alumina	Alcoa	500	360
BPL Carbon	Calgon Carbon	540	1100
Silica Gel	Davison	430	800
Zeolite 13X	UOP	240	690

Activated alumina is an amorphous form of aluminum oxide. Controlled dehydration (calcining) is used to produce the hydrated form $Al_2O_3 \cdot nH_2O$ where n is approximately 0.5. The crystalline forms of alumina can exhibit high catalytic activity as a result of surface defects in the crystal matrix. However these forms are less effective as adsorbents due to low surface area. The presence of terminal surface hydroxyl groups with acid character results in a high affinity of the alumina adsorbent for water adsorption. Activated alumina is often used as a desiccant because it is stable in the presence of liquid water. Figure 5 presents the surface structure of alumina. The pKa of the surface hydroxyl group is reported to be 3.2.

Silica gel is another adsorbent, which is much used as a desiccant. The surface area and water capacity are typically greater than alumina. It is derived as a dehydrated form of silicon oxide. It consists of microparticles of colloidal silica. Terminal hydroxyls lead to favorable water vapor adsorption, which requires conditions of approximately 200 °C for regeneration. Contact of silica gel with liquid water can lead to collapse of the porous structure. Many forms of silica are available which offer different choices in pore size and particle size. Zeolite molecular sieves have wide applicability as desiccants and for permanent gas separation. Activated carbon provides a less active non-polar character with can be prepared in highly activated form of 60% void volume.

2. EXPERIMENTATION

2.1 Adsorbent Sample Preparation.

The adsorbents selected for this study were obtained commercially. Both dried and humidified samples were prepared. The adsorbent was then introduced to the sample tube along with the chemical. Subsequently the sample tubes were loaded into the NMR spectrometer for analysis. The sample analysis was performed at a rate required to capture the observed transient behavior.

Each of the adsorbents considered had unique properties of shape, texture, and adsorption affinity. Some of the properties of the samples are listed in Tables 3 and 4. The alumina used in this study was obtained from Alcoa Industrial Chemicals (Vadilia, LA), in the form of 2.0 mm beads. The adsorbent can be pretreated by heating it to 250 °C to desorb water. The silica adsorbent used in the present work was supplied by Davison Division, W.R. Grace, Inc. (Baltimore, MD). It is grade 40 supplied as 6-12 mesh, which was crushed and sieved to 18 x 25 mesh.

Table 4. Adsorbent Conditions

	Particle Size	Particle Diameter (mm)	Water Loading (g/g)	Drying Temperature
Alumina	7x14	2.0	0.165	250 °C
BPL Carbon	12x30	1.0	0.388	110 °C
Silica Gel	18x25	0.84	0.281	250 °C
Zeolite 13X	16x20	1.0	0.258	350 °C

To establish to conditions of each adsorbent a regeneration step was first performed. Exposure to ambient concentrations of water vapor results in moisture pickup. Therefore each adsorbent sample was first dried overnight. The drying temperatures are listed in Table 4. The samples were dried under temperature conditions, which depend on the strength of adsorption of water vapor. For the cases with humidified samples humidification was performed at 80% relative humidity and 25 °C by placing samples in an environmental chamber through which humid air was circulated. Small samples of adsorbent will be dried and weighed to confirm the water loading.

The sample consisting of several particles will then be weighed to approximately 200 mg then loaded in an NMR rotor tube. Due to variations in particle size and density the number of particles varies in each case. The dimensions of the tube are 6.7 mm outer diameter and 23.9 mm length. The chemical mass is then measured by weight difference using a liquid syringe. The dose of 10 wt % chemical or approximately 20 µl is delivered to the NMR rotor containing the adsorbent particles.

2.2 Solid Phase NMR Analysis Technique.

A Varian INOVA 400 operating at 400 M Hz was used for this study. It was equipped with a Doty Scientific 7 mm Supersonic VT-MAS solids probe. The sensitivity of these measurements is approximately 1%.

The rotor will be analyzed at periodic intervals. All prepared NMR rotor samples will be stored in an oven at 50 °C. The sample will be taken from the oven and analyzed at room temperature.

This work will examine ^{13}C for mustard (isotopically labeled with ^{13}C); and ^{31}P MAS NMR for VX, GD, and GB; and C^{13} for HD and acetic anhydride. The external reference was H_3PO_4 (0 ppm) for ^{31}P, TMS (0 ppm) for ^{13}C for HD and $CDCl_3$ (77 ppm) for acetic anhydride. The approximate signal range for each species is listed in Table 5, while the natural abundance of each isotope is listed in Table 6.

Table 5. NMR Signal Range

GD	^{31}P	2x integral of (32 - 35 ppm)
HD	^{13}C	2x [integral of (34 - 36 ppm) – integral of (26 – 28 ppm)]
VX	^{31}P	integral of (52 – 62 ppm)
GB	^{31}P	2x integral of (0 – 60 ppm)
AAh	^{13}C	2x [integral of (34 - 36 ppm) – integral of (26 – 28 ppm)]

Table 6. Isotope Natural Abundance

^{1}H	-	99.9%
^{13}C	-	1.1%
^{31}P	-	100%

3. RESULTS AND DISCUSSION

3.1 Behavior of HD on Adsorbents.

The transient behavior of ^{13}C labeled HD, applied drop-wise to an adsorbent sample, was observed by NMR equipped with a solid probe. The NMR spectrum was analyzed to quantify the rates of chemical reaction and adsorption.

Figure 6 presents the spectrum 1 hr after introduction of the HD to the silica gel sample. Two principle peaks are observed at 35 and 44 ppm. The integrated signal response for each peak is overlaid in this figure. The chemical shifts for HD are 35.8 and 45.0, see Table 6. The fact that both peaks do not integrate to exactly the same height is a result of an impurity, $CH_3(O)OCH_2CH_2S\text{-}CH_2CH_2Cl$, of approximately 8%. The total HD signal is taken as twice the area of the 35.8 ppm peak. Alternatively twice the area of the 45.0 ppm peak could be used however it can be seen in Table 7 that the sulfonium ion with a peak at 28.6 is present in the spectrum, which has a corresponding peak at 44.2. Therefore the area at 45.0 ppm must be corrected by subtracting an equivalent area corresponding to the second sulfonium ion peak of 44.2 ppm. The latter had combined in the integration of the HD peak.

Table 7. NMR Parameters of HD and Hydrolysis Products

	HD	CH-TG	H-2TG	TG
$S^{13}CH_2CH_2Cl$	35.8			
$SCH_2{}^{13}CH_2Cl$	45.0			
$S^{13}CH_2CH_2OH$		36.3		36.2
$SCH_2{}^{13}CH_2OH$		63.2		63.2
$^{+}S^{13}CH_2CH_2OH$		46.4	46.4	
$^{+}SCH_2{}^{13}CH_2OH$		59.0	59.0	
$S^{13}CH_2CH_2S^{+}$		28.6	28.6	
$SCH_2{}^{13}CH_2S^{+}$		44.2	43.8	

Shown in Figures 7 and 8 are the spectra recorded at 6.25 and 24.25 hr. The disappearance of the peak at 35 ppm by 24 hr indicates complete reaction of the original HD, while the presence of the peak at 45 ppm indicative of the sulfonium ion product. The total signal obtained by adding the area of all the peaks at 24 hr corresponds to 251 while the signal obtained at 60 min gave a total peak area of 360 units. The loss of ^{13}C response results from evaporation of product. The area "loss" is most likely due to longer T1's of the products.

Extraction of the HD silica sample with hexane was performed. The extract was analyzed using ion chromatography/mass spectrometry. Three species were identified using including HD, thioxane, and thioxine in a ratio of 27, 22, 51 %.

The reaction of HD on humid activated alumina is presented in Figure 9. After 1 hr at 50 °C product can be detected in the spectrum, by 6 hr the sample is 50% consumed and by 24 hr there is no detectable HD. All three of the products listed in Table 7 can be identified in the spectrum at 24 hr. Similar observations can be made for HD on humid 13X zeolite. The results for dry 13X are listed in Figure 10 after 1 hr the sample indicates a broad peak overlaying the ^{13}C HD peaks indicating the presence of significant reaction products. The peak area for HD is determined by constructing tangents from the peak maximum to the baseline then evaluating the height difference of the integration curve as it passes between the two tangent lines. This result indicates that only 17% of the starting mass remains after 1 hr. The more rapid reaction on dry 13X is a result of greater available pore volume due to less adsorbed water than for the humidified case. The HD does not appear to have reacted to completion after 72 hr. A final spectrum was evaluated after 21 days. It was not possible to determine the presence of HD with this sample because the product peaks overlay the HD peaks.

It is interesting to note that the NMR spectrum obtained on dry BPL sample shows a shift for the two HD peaks 35 to 29 ppm and 45 to 38 ppm. This results from the greater porosity of BPL activated carbon than the other adsorbents allowing more extensive penetration and the presence of the carbon matrix of BPL itself. No observable HD reaction is noted even after 7 days in the dry case at 50 °C. For the case of HD on humid BPL carbon again the shift in peak placement is noted. After 6 hr approximately 60% of HD remains unreacted while at 24 hr complete hydrolysis has occurred. The thiodiglycol appears to be the primary product, where its peaks have shifted to 29 and 56 ppm. Due to the strong sensitivity of HD reaction to adsorbed water an additional series of experiments would be valuable to characterize the relationship between water loading and HD hydrolysis rate.

3.2 Behavior of GD on Adsorbents.

The NMR spectrum for GD after 1 hr on silica is shown in Figure 11. Four peaks of the GD spectra result from an equal distribution of two GD isomers and fluorine splitting of each of those two isomers. The liquid or weakly adsorbed phase is represented by 26.4, 27.2 and 32.8 and 33.6 ppm peaks. Chemical shifts associated with surface bound adsorption are also noted in Figure 11. There are two forms of surface bound products also represented in Figure 11. These two products are shown in Figure 12. The bidendate structure appears as an intermediate corresponding to peaks at 34.7 and 34.1 ppm. This eventually reverts to the monodentate form as seen at 29.5 and 28.2 ppm with the disappearance of the bidentate species. Reaction of GD either with the surface or adsorbed water cleaves the fluorine.

The first spectrum was recorded at 1 hr and it can be seen that significant chemical reaction has occurred due to the presence of product peaks. By 6 hr the reaction of GD has gone to completion and indicated by the disappearance of the 32.9 ppm peak. At 24 hr only a single broad peak remains, from which it is not possible to distinguish the various product species. It can be noted that the splitting of the phosphorous peak due to fluorine is no longer apparent once the fluorine group leaves after 6 hr.

Similar results are observed for GD on alumina, both humid and dry 13X, and humid BPL where reaction had gone to completion by the time of the second recorded spectra at 6 hr. For GD on dry BPL carbon broad peaks associated with adsorption as shown if Figure 13 with shifts due to micropore adsorption at 19.0 and 25.1 ppm. The fluorine splitting is not evident. Reaction occurs to approximately 50 % after 5 hr with no discernable reaction product peaks.

3.3 Behavior of VX on Adsorbents.

The ^{31}P NMR spectrum for VX is characterized by a single peak at 59 ppm while as a liquid the VX peak appears at 54 ppm. The result obtained for VX on silica gel after 1 hr is seen in Figure 14. A second larger peak at 26.5 ppm corresponds to the hydrolysis product EMPA. The second spectrum obtained at 6 hr indicates that the conversion of VX to EMPA is complete. The sum of the peak area obtained at 6 hr and 1 hr do not agree exactly representing some loss of material in the baseline or evaporation.

VX on alumina does show an initial presence of the liquid and less amount of product after 1 hr. By 6 hr more product is present, and by 24 hr the conversion is complete. VX on humid 13X indicates the presence of product at 24 hr and only complete conversion after 48 hr. On dry 13X the shift of VX occurs and 50.8 ppm due to diffusion into the pores of the binder. The conversion is complete after 24 hr.

Reaction of VX on wet BPL is complete after 1 hr, which may be favored by the rapid diffusion through the larger pores of BPL. On dry BPL again a broad adsorption peak is observed at 49 ppm which is shifted from the peak at 59 noted with silica gel. Reaction goes to completion after 24 hr. It is noted that VX tends to exhibit a autocatalytic behavior which promotes reaction even under dry conditions.

3.4 Behavior of GB on Adsorbents.

Measured rate behavior for GB was obtained on BPL activated carbon. Earlier work had examined GB adsorption on coconut shell carbon (Karwacki et al. 1999b) Under humid conditions complete reaction proceeded by the time the first spectra was collected at 1 hr (Figure 15). In the absence of adsorbed water, hydrolysis is not observed. The spectrum in Figure 16 was obtained immediately after preparation of the sample tube with GB on dry BPL. As with GD two peaks are present at 24 and 18 ppm corresponding to the two isomers on phosphorous. The presence of spinning side bands for each peak is also apparent. There is no conversion of GB observed for this sample for a period up to 28 days. The non-polar characteristic of the surface and the absence of adsorbed water allows the sample to remain un-reacted.

3.5 Behavior of Acetic Anhydride on Adsorbents.

A sample for solids analysis was prepared using 10 wt% acetic anhydride on humidified silica gel. There is a level of background response for carbon due an o-ring in the rotor. Using TMS as an external reference this peak appears at 106 ppm. The spectrum for the

acetic anhydride on silica gel at 45 min is seen in Figure 17. There are two peaks corresponding to acetic anhydride at 21 and 168 ppm and two peaks for acetic acid at 20 and 176 ppm.

3.6 Reaction Rate Analysis.

The observed loss of starting chemical and product formation through the NMR studies can be quantified in term of reaction rate. However due to the multiphase aspects of this problem the adequacy of a simple model must be considered first. Concentrations of the starting chemical are distributed between the pellet internal and external geometry and with the water adsorption partially filling the adsorbent pores. Earlier studies considering adsorption and reaction have relied on evaluation of a first order rate in terms of the starting component.

The measured NMR spectra can be analyzed using the integration routines. The integrated peak height was measured for the starting species for each spectrum. A rate constant was determined from a minimum of two data points. It is also instructive to report this rate in terms of a reaction half time. In addition the total integrated response is determined from each spectrum. In some cases there can be loss of signal during the course of the run. The results for each adsorbate/adsorbent pair is listed in Table 8.

Table 8. First Order Reaction Half-Time and Rate Constants

Chemical	Adsorbent	Dry/Humid	k (min^{-1})	Halftime (min)	Non-Zero Data Pts.
HD	silica	humid	$5.5x10^{-3}$	125	3
HD	alumina	humid	$2.7x10^{-3}$	254	3
HD	13X	humid	$2.6x10^{-3}$	267	3
HD	13X	dry	$2.9x10^{-2}$	24	5
HD	BPL	humid	$1.6x10^{-3}$	439	3
HD	BPL	dry		>10000	3
GD	silica	humid	$7.0x10^{-3}$	99	2
GD	alumina	humid	$3.7x10^{-2}$	19	2
GD	13X	humid	$4.8x10^{-3}$	144	2*
GD	13X	dry	$4.8x10^{-2}$	14	2
GD	BPL	humid		<60	1
GD	BPL	dry	$1.9x10^{-3}$	363	3*
VX	silica	humid	$4.0x10^{-2}$	17	2
VX	alumina	humid	$1.0x10^{-2}$	60	3
VX	13X	humid	$9.5x10^{-4}$	728	4
VX	13X	dry	$2.8x10^{-3}$	249	3*
VX	BPL	humid	$6.1x10^{-2}$	11	2
VX	BPL	dry	$1.1x10^{-3}$	644	3*
GB	BPL	humid		<60	1
GB	BPL	dry	$8.7x10^{-2}$	>40000	2
Acetic Anhydride	silica	humid	$7.1x10^{-3}$	100	11

*indicates autocatalytic behavior

The reaction half-time determined for HD is fairly consistent for all except two cases: dry 13X and BPL. The other cases considered were all humid ranging from 125-439 min for each adsorbent silica, alumina, 13X and BPL. Each of these cases corresponds to a high water loading leading to competitive adsorption. The dry BPL results are consistent with the results reported earlier for HD decomposition on coconut shell carbon (CSC), where the HD was shown to be stable when no water is present even up to 100 °C. When water was present on CSC the reported reaction half times were 25 and 9.5 days at 30 and 60 °C respectively, whereas the current findings indicate a half time of 0.3 days at 50 °C on humid BPL carbon. The reason for the more rapid reaction for the present conditions is likely due to the higher water loading 0.388 g/g in the present work with BPL carbon versus 0.13 g/g in the work with CSC. This agreement is obtained regardless of the method of introducing the adsorbate as a vapor or a liquid in the present case. Rapid reaction on dry 13X molecular sieve is observed and would probably also occur on dry silica gel and dry activated alumina although the latter two cases were not measured. The reason is that the13X would have been slightly hydrated upon processing in ambient air while prepped in the NMR rotor tube.

In general, the reaction rates of HD are observed to be somewhat slower than for GB, GD and VX. One exception is that HD and GD react more rapidly than VX on 13X. This is probably a result of the size of HD and GD being able to fit into the 13X cage while VX would be excluded resulting in vastly different reaction times. In contrast the large pores of BPL allow rapid reaction of VX under humid conditions. HD reaction on humid BPL is somewhat slower than on silica, alumina and 13X.

Silicon and aluminum oxides have amorphous structures with the formula SiO_2 and Al_2O_3 respectively. Surface hydroxyl groups, Figure 15, tend to act as acids which can react with adsorbed species and promote hydrolysis. This can lead to faster observed decomposition than on a non-polar adsorbent such as activated carbon. Molecular sieve 13X is even more reactive than silica and alumina because it has a charge in the crystal framework due to the valence difference between silicon and aluminum which is balanced by the presence of cations with the formula, $Na_{86}[(AlO_2)_{86}(SiO_2)_{106}]\cdot 276H_2O$. The zeolite cage can act effectively as a Lewis acid or base while achieving a close fit with adsorbed molecules.

There are many of the cases studied that the reaction rate was not well characterized. Table 8 lists the number of non-zero concentration data points obtained for each run. Figure 18 presents the results for HD on alumina, which shows good agreement between model and data. In contrast, the reaction of VX is known to be autocatalytic, i.e., catalyzed by product formation. The fluorine-leaving group tends to make the solvent more acidic, which promotes further hydrolysis. The rate would be slow initially but then progress rapidly. This is demonstrated in Figure 19 where no product is formed up to 500 min but the reaction goes to completion by 1400 min. On the humid adsorbent reaction occurs by hydrolysis with excess water. This autocatalytic behavior illustrated on dry BPL is also observed on several other samples as noted in Table 8. In other cases where it may be occurring with the phosphonates there may not have been enough data points recorded to observe it.

Acetic anhydride reaction is characterized by a half-time of 100 min, which contrasts with the value of 8 min in solution reported by Asprey. The concentration of acetic anhydride for the humid silica experiment corresponds to 2.59 mol/l relative to the amount of adsorbed water, while an initial acetic anhydride concentration of 0.89 mol/l was reported for the liquid phase experiments of Asprey. Based on the results in Table 7, acetic anhydride appears to react at a rate, which may make it useful and a simulant of the chemical agents. The stability of acetic anhydride as a vapor in contact with various other materials such as sampling lines would have to be considered further and compared to the behavior of the chemical agents.

The rates determined using the solid phase technique are slower than pure component vapor phase diffusion rates for adsorption systems. The latter occur with a time constant of approximately 1 s. The observed immediate uptake on dry BPL is supportive of this conclusion. The fastest NMR MAS spectra that can be recorded on BPL, e.g., GB dry on BPL Figure 16, indicate immediate shifting of peaks corresponding the adsorbed environment.

The adsorbed phase reaction can be either faster or slower than the corresponding liquid phase reaction. Acetic anhydride on silica is shown to be slower, while HD reaction on BPL carbon is more rapid than in solution. This appears to be related to liquid phase solubility. The low water solubility of HD can be effectively increased in the adsorbed phase by providing a greater surface area for contact. This is consistent with the effect of drop size reported earlier. A more comprehensive literature review would be valuable in comparing the extent of this effect.

4. CONCLUSIONS

Experiments were conducted to quantify the reaction rates associated with the chemical warfare agents HD, GD, GB and VX on high surface area adsorbents. Results were obtained by recording the loss of signal of the starting material using solid phase NMR. Samples of silica gel, alumina, BPL activated carbon and 13X molecular sieve were pre-equilibrated at 80% relative humidity, while 13X and BPL activated carbon were also examined under dry conditions. The chemical was applied to the sample as a liquid drop in the rotor.

Complete disappearance was noted for all cases except dry BPL carbon. The loss of material is taken to associated with chemical reaction because hydrolysis product peaks can be identified in most cases. The reaction rate expressed as a half-time ranged from 10 to 400 min for most samples.

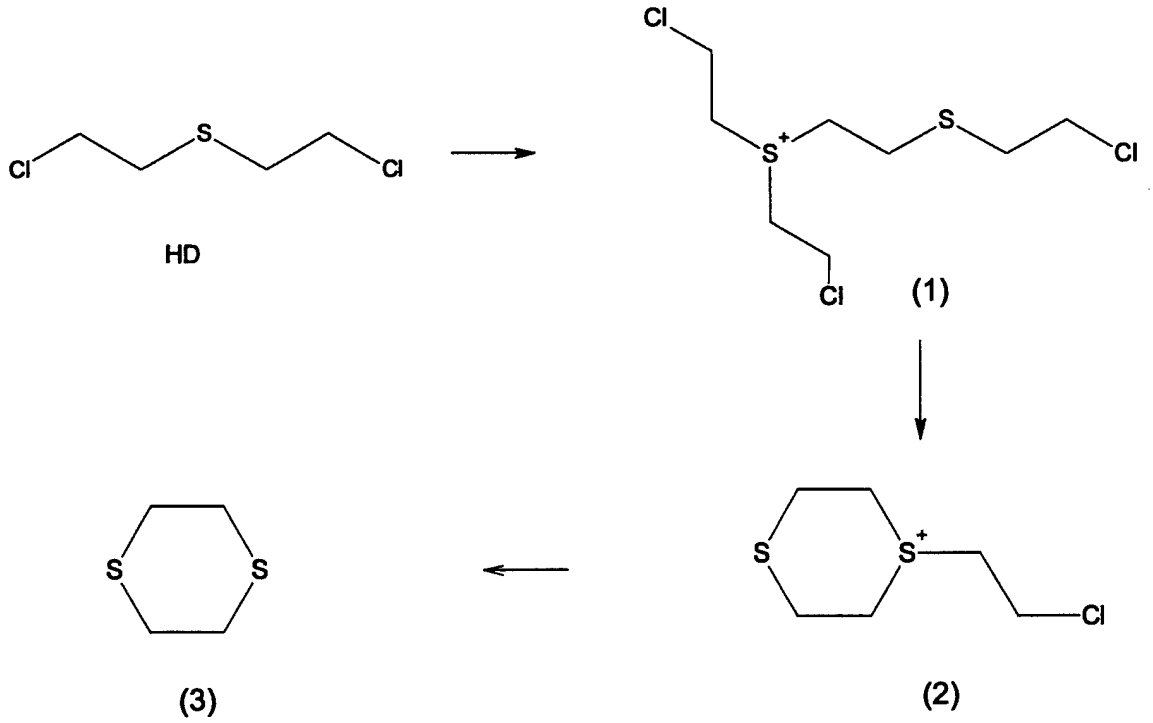

Figure 1. Hydrolysis Products Formation for HD.

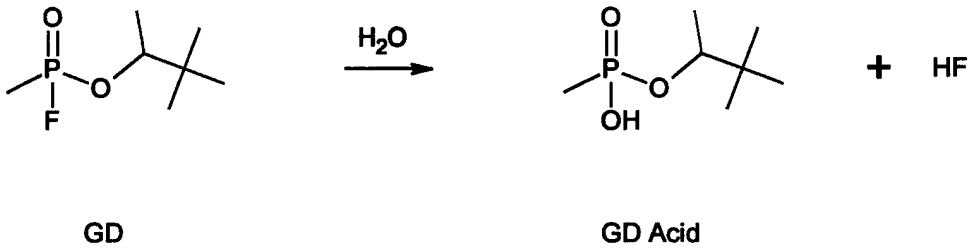

Figure 2. Hydrolysis Products of GD.

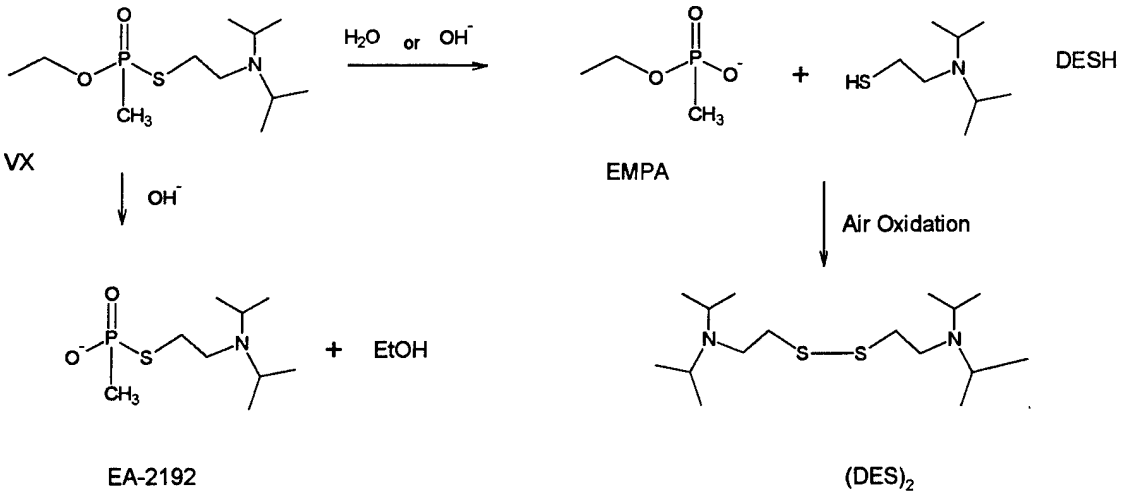

Figure 3. Hydrolysis Products of VX.

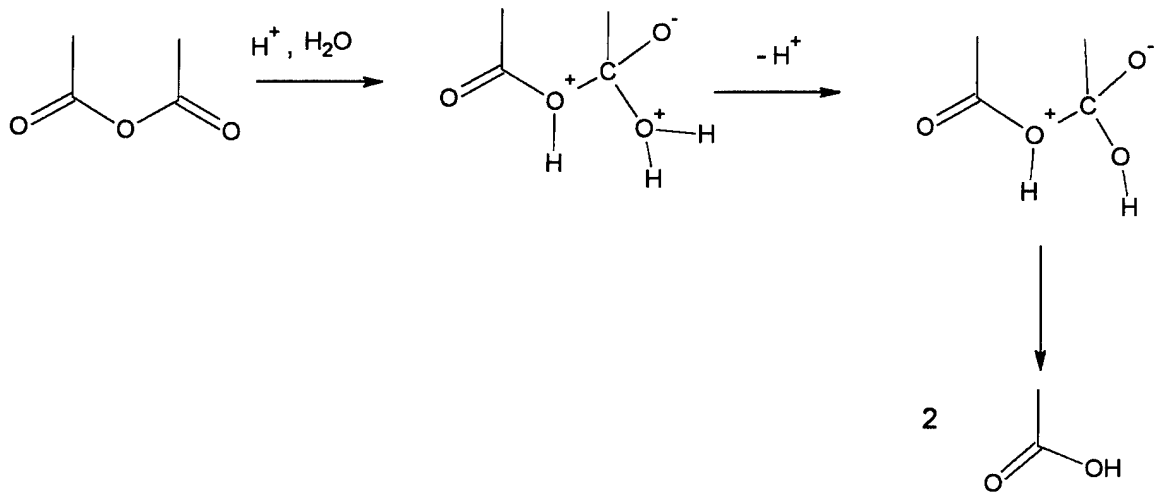

Figure 4. Hydrolysis Products of Acetic Anhydride.

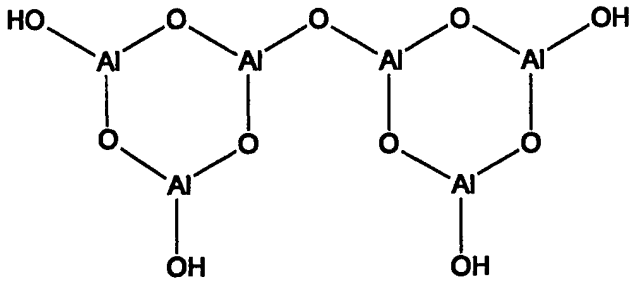

Figure 5. Al_2O_3, Showing Surface Hydroxyl Groups.

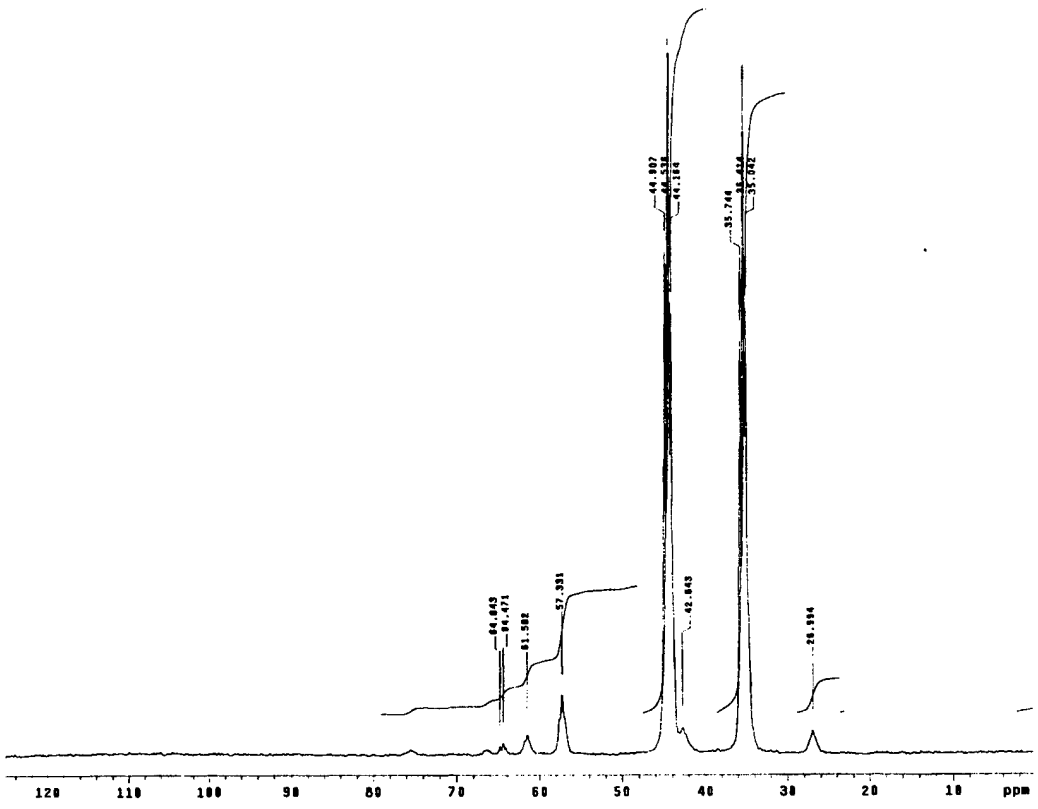

Figure 6. NMR Spectrum of HD on Humid Silica Gel at 1 hr.

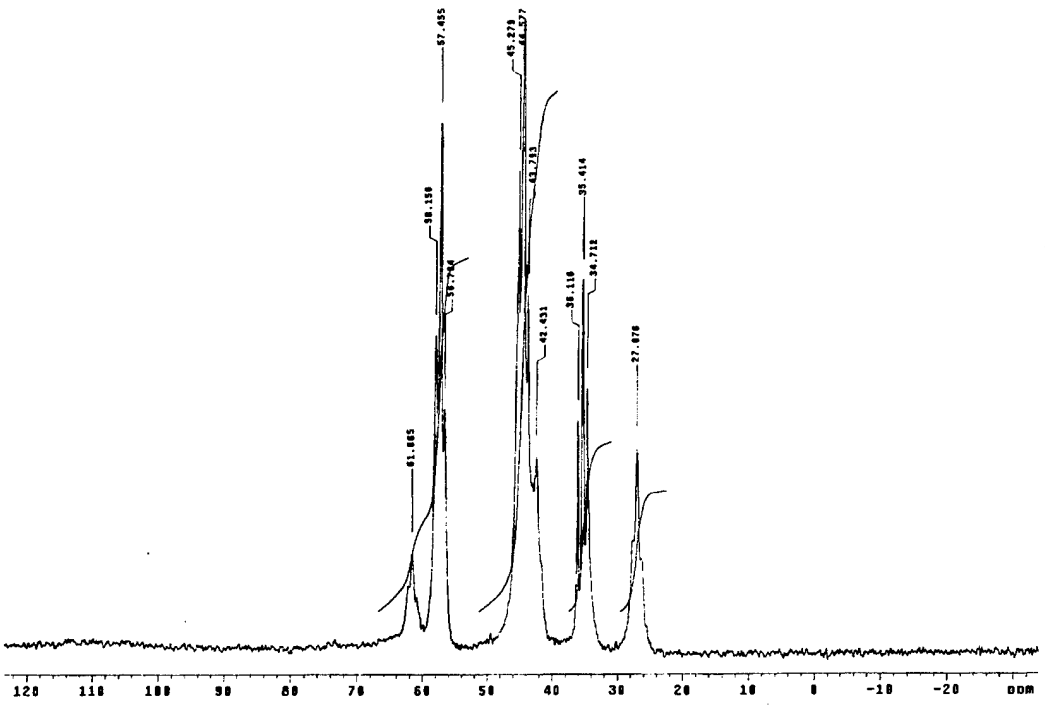

Figure 7. NMR Spectrum of HD on Humid Silica Gel at 6.25 hr.

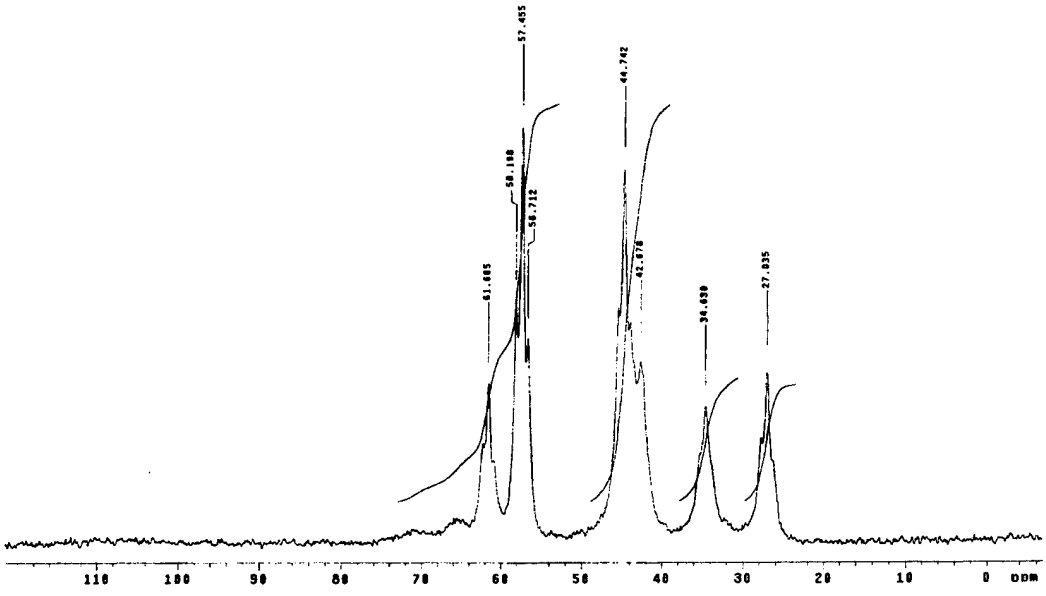

Figure 8. NMR Spectrum of HD on Humid Silica Gel at 24 hr.

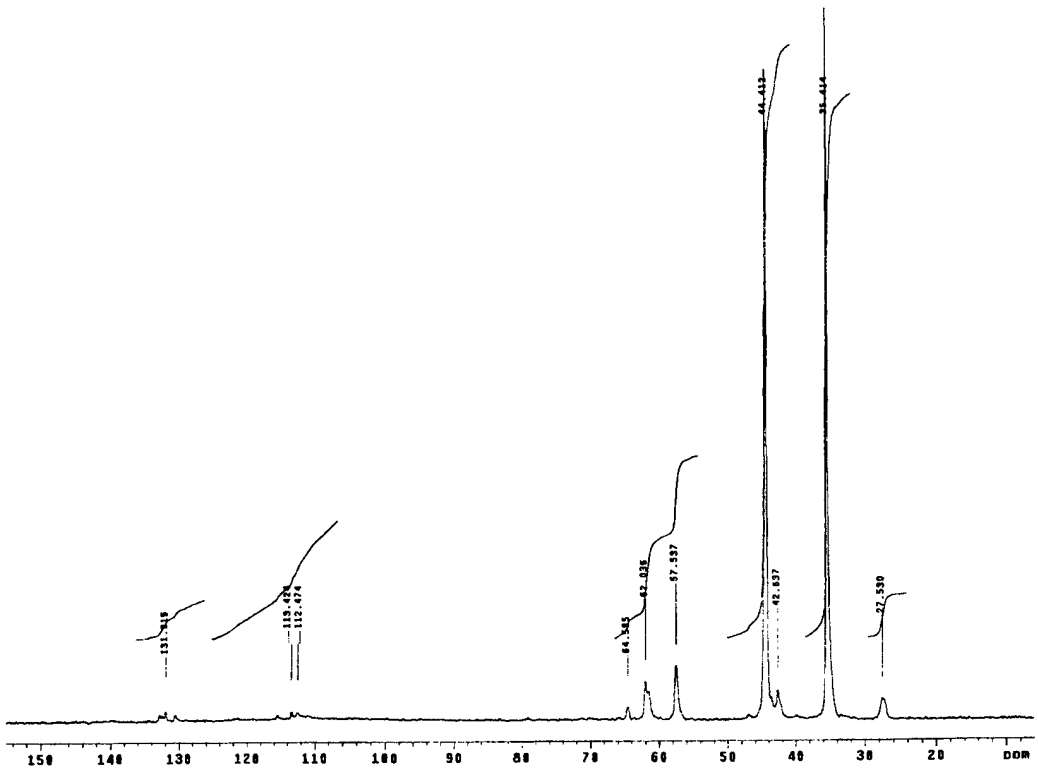

Figure 9. NMR Spectrum of HD on Humid Alumina at 1 hr.

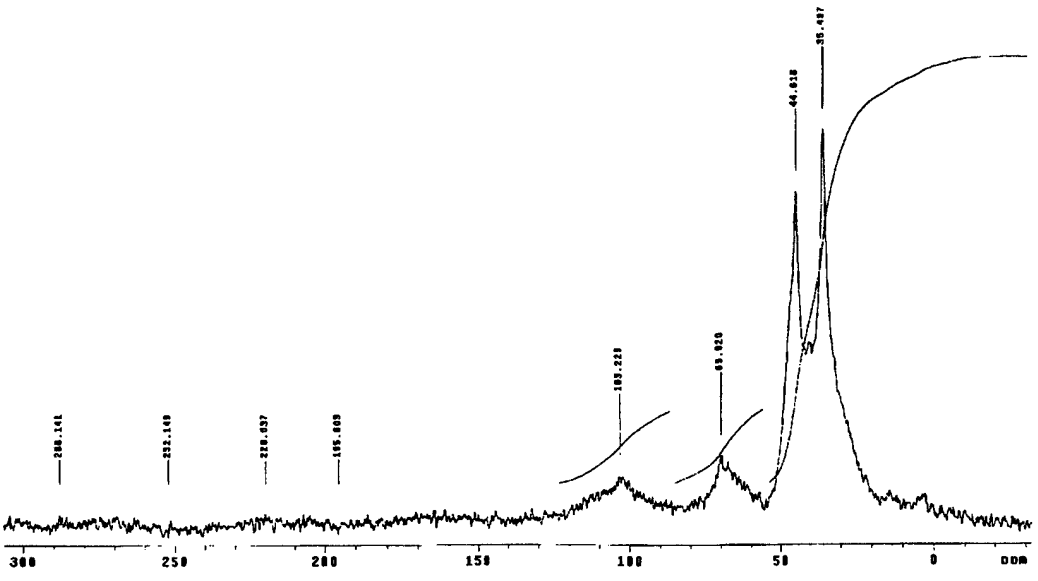

Figure 10. NMR Spectrum of HD on Humid Zeolite 13X at 1 hr.

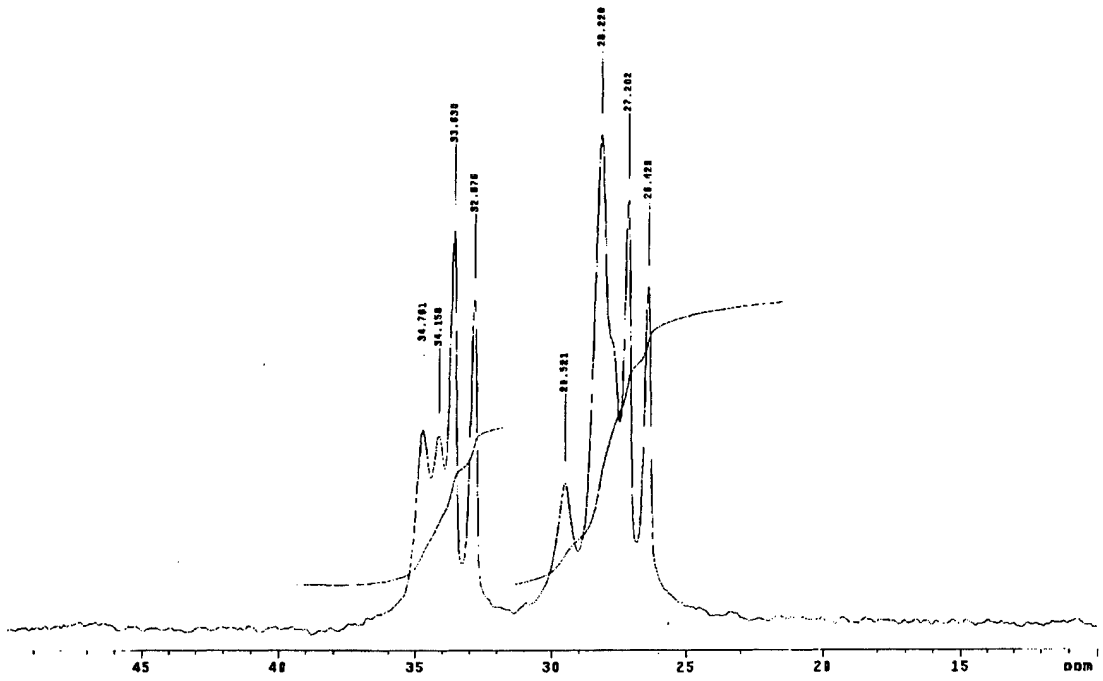

Figure 11. NMR Spectrum of GD on Humid Silica Gel at 1 hr.

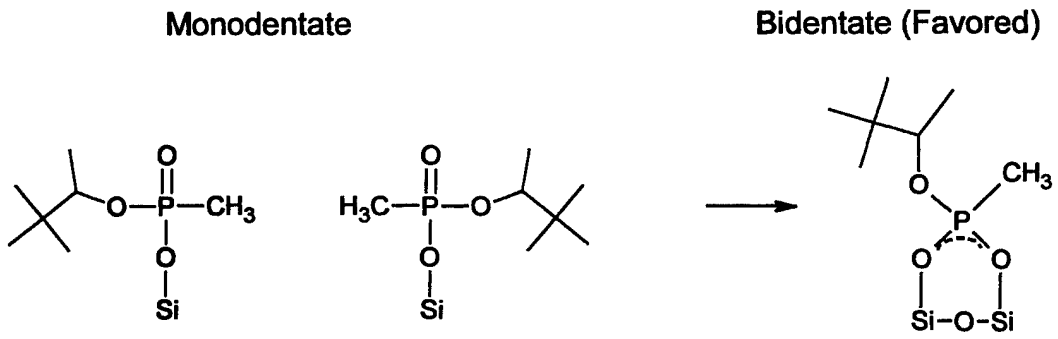

Figure 12. Hydrolysis Products Formation for GD, Adsorbent Bonding of GD on Silica Surface, Monodendate and Bidendate.

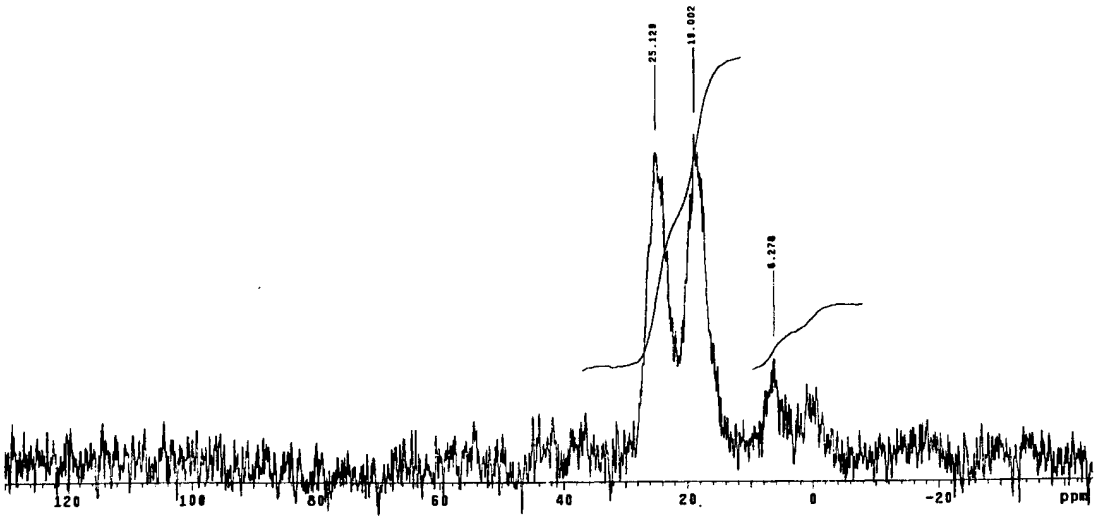

Figure 13. NMR Spectrum of GD on Dry BPL at 1 hr.

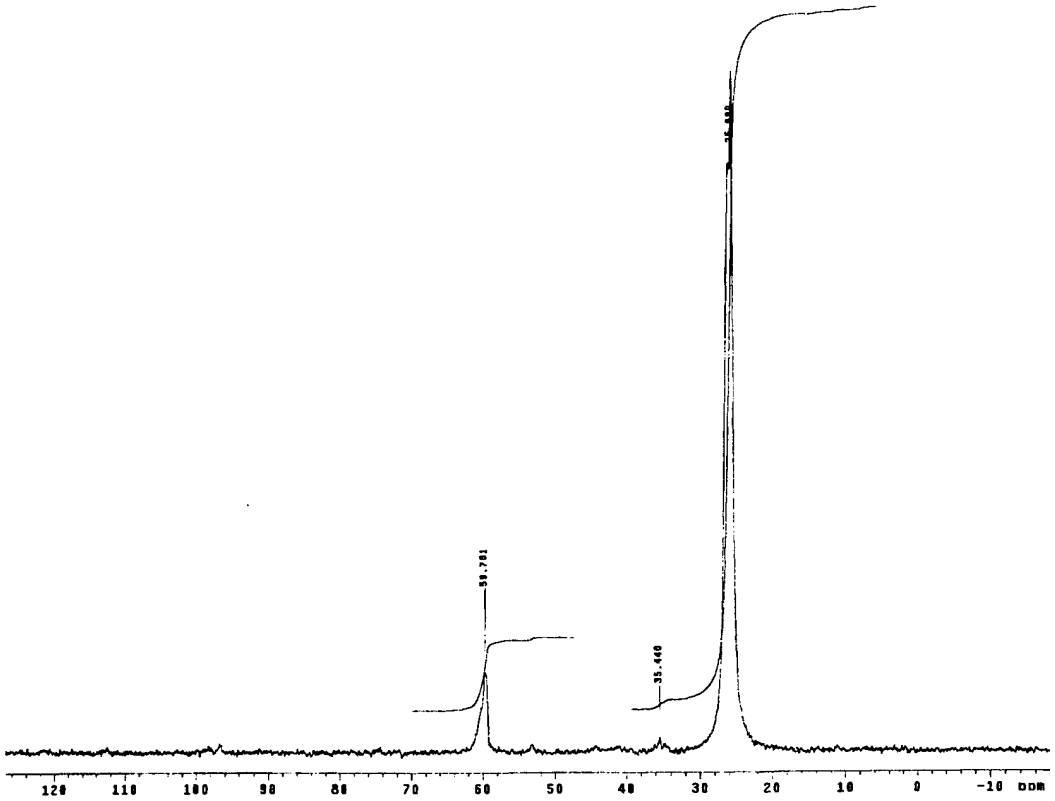

Figure 14. NMR Spectrum of VX on Humid Silica Gel at 1 hr.

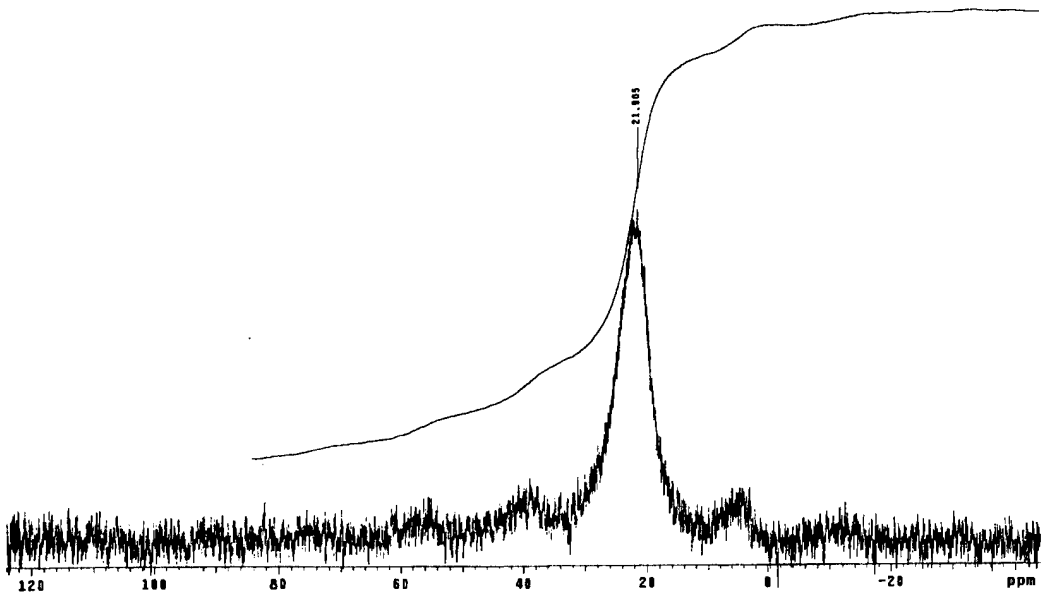

Figure 15. NMR Spectrum of GB on Humid BPL Carbon at 1 hr.

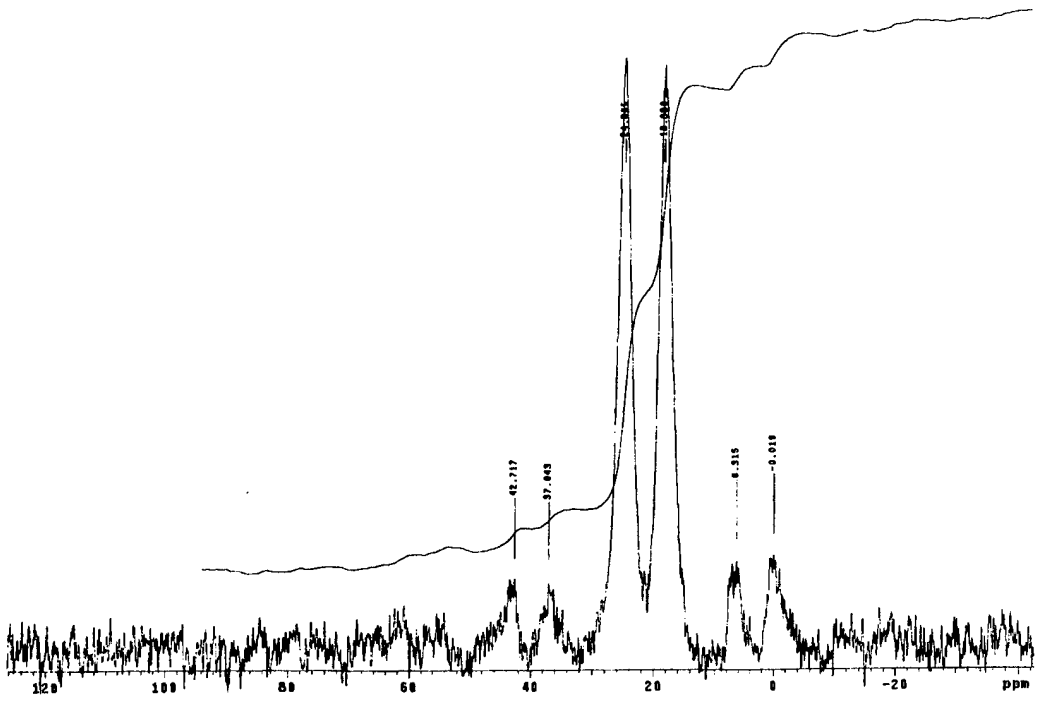

Figure 16. NMR Spectrum of GB on Dry BPL Carbon at Start.

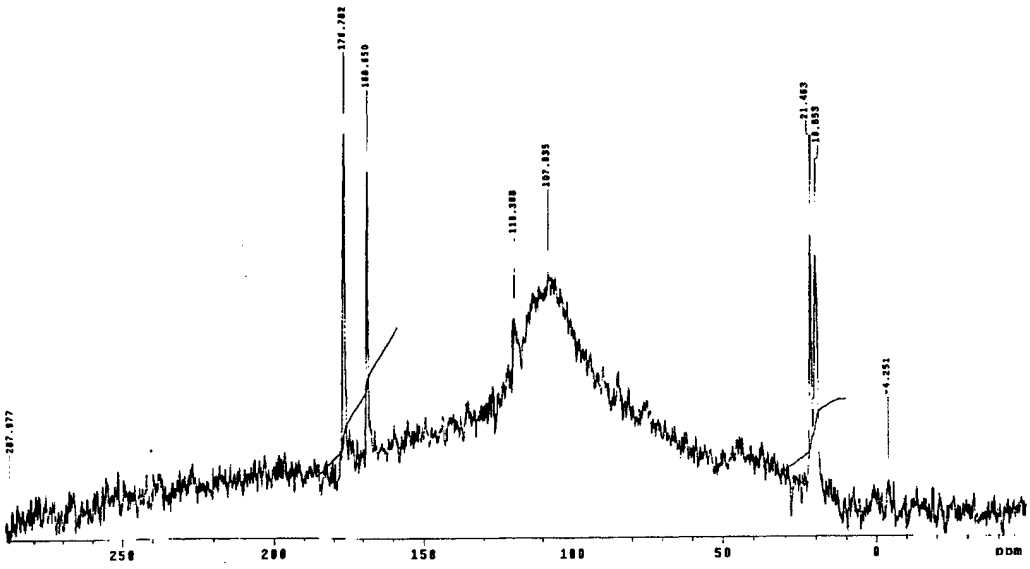

Figure 17. NMR Spectrum of Acetic Anhydride on Silica Gel at 45 min.

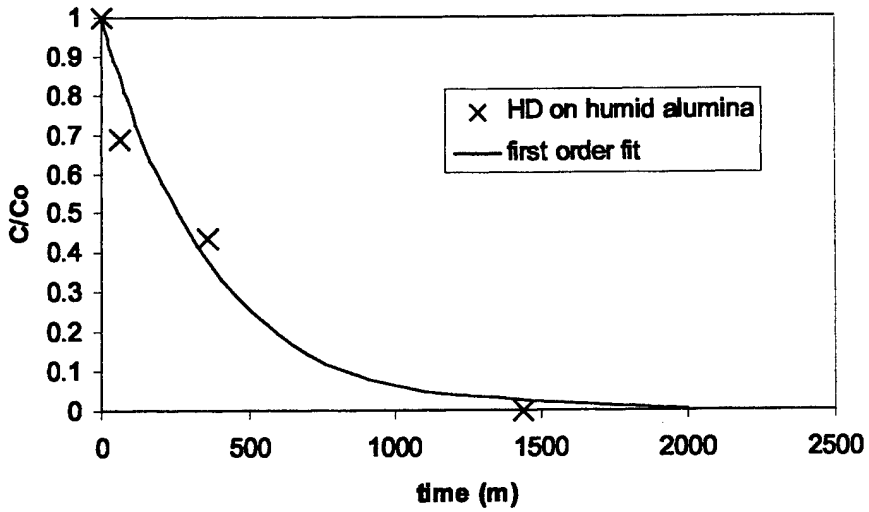

Figure 18. Reaction Rate Behavior of HD on Humid Alumina Demonstrating First Order Behavior.

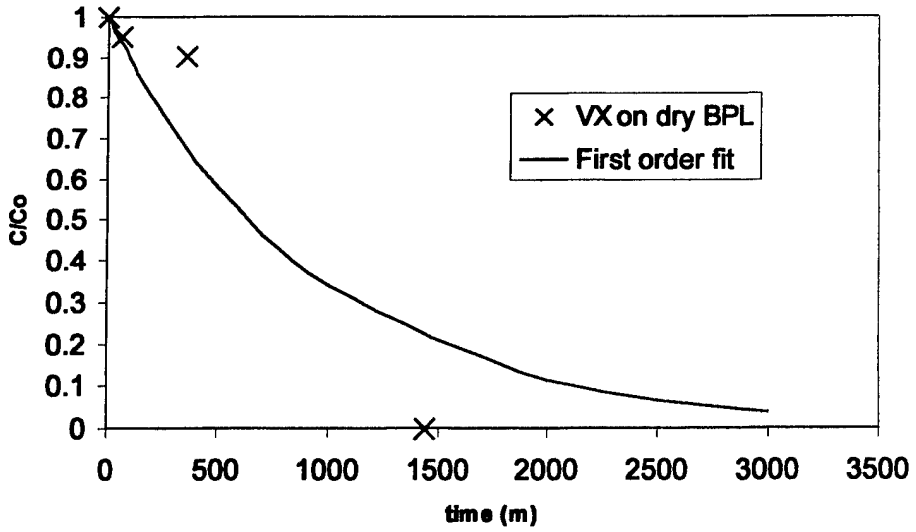

Figure 19. Reaction Rate Behavior of VX on Dry BPL, Demonstrating Autocatalytic Behavior.

LITERATURE CITED

1. Wagner, MacIver, Yang "Magic Angle Spinning NMR Study of Adsorbate Reactions on Activated Charcoal," Langmuir, 11(5), 1439, 1995.

2. Karwacki, C.J., Buchanan, J.H., Mahle, J.J., Buettner, L.C., Wagner, G.W., "Effect of Temperature on the Decomposition of Mustard from Activated Carbon," Langmuir, 15, 8645, 1999a.

3. Yang, Y., Szafraniec, L.L., Beaudry, W.T., and Ward, J.R., "Kinetics and Mechanism of the Hydrolysis of 2-Chloroethyl Sulfides," J. Org. Chem., 53(14), 3293-3297 (1988).

4. Asprey, "Applications of Temperature Scanning in Kinetic Investigations of the Hydrolysis of Acetic Anhydride," Chem. Eng. Sci., 51(20), 4681, 1996.

5. Wagner, G.W., Procell, L.R., and Munavelli, S., "^{27}Al, ^{47,49}Ti, ^{31}P, and ^{13}C MAS NMR Study of VX, GB, GD and HD Reactions with Nanosize Al_2O_3, Al_2O_3, TiO_2, Aluminum and Titanium," ECBC-SP-015, In Proceedings of the 2002 Joint Services Scientific Conference on Chemical and Biological Defense Research, 19-21 November 2002, July 2003.

6. Karwacki, Tevault, Mahle, Buchanan, Buettner, "Adsorption Equilibria of Isopropyl Methylphosphonofluoridate (GB) on Activated Carbon at Ultralow Relative Pressures," Langmuir, 15(9), 6343, 1999b.

7. Wagner, G., MacIver, B., Karwacki, C., Buchanan, J., Rohrbaugh, D. "Fate of Mustard on Activated Carbons Part 2. ^{13}C MAS NMR Studies," In Proceedings of the 1997 ERDEC Scientific Conference on Chemical and Biological Defense Research, pp 173-179, July 1998.